Article:

Ivanovic, RF orcid.org/0000-0002-7805-6018, Flecker, R, Gutjahr, M et al. (1 more author) (2013) First Nd isotope record of Mediterranean–Atlantic water exchange through the Moroccan Rifian Corridor during the Messinian Salinity Crisis. Earth and Planetary Science Letters, 368. pp. 163-174. ISSN 0012-821X

https://doi.org/10.1016/j.epsl.2013.03.010

First Nd isotope record of Mediterranean-Atlantic water exchange through the Moroccan Rifian Corridor during the Messinian Salinity Crisis

Authors and affiliations

Ruza F. Ivanovic[a], Rachel Flecker[b], Marcus Gutjahr[c], Paul J. Valdes[d]

[a]Corresponding author: School of Geographical Sciences, University of Bristol, University Road, Bristol, BS8 1SS, UK; Ruza.Ivanovic@bristol.ac.uk. Tel: +44 117 331 7313, fax: +44 117 928 7878

[b]School of Geographical Sciences, University of Bristol, University Road, Bristol, BS8 1SS, UK; r.flecker@bristol.ac.uk

[c] GEOMAR Helmholtz Centre for Ocean Research Kiel, Wischhofstrasse 1-3, 24148 Kiel, Germany; mgutjahr@geomar.de

[d]School of Geographical Sciences, University of Bristol, University Road, Bristol, BS8 1SS, UK; p.j.valdes@bristol.ac.uk

Abstract

We present the first neodymium isotope reconstruction of Mediterranean-Atlantic water exchange through the Moroccan ('Rifian') Corridor 8 to 5 Ma. This covers the late Miocene Messinian Salinity Crisis (MSC); a period when progressive tectonic restriction of the Mediterranean-Atlantic seaways resulted in extreme, basin-wide Mediterranean salinity fluctuations. The Rifian Corridor was one of these seaways and until now, relatively poor age constraints existed for the timing of Corridor closure, due to the impact of uplift and erosion on the sedimentary record. The bottom water Nd isotope record from the continuous Bou Regreg Valley succession in northwest Morocco allows us to explore corridor connectivity with the Atlantic. Data from the interior and Mediterranean edge of the Rifian Corridor (respectively, the Taza-Guercif and Melilla basins, northern Morocco) provides new information on corridor shallowing and the provenance of water flowing through the seaway. As a result, we can constrain the age of Rifian Corridor closure to 6.64-6.44 Ma. We also find no evidence of the siphoning of Atlantic waters through the seaway (7.20-6.58 Ma). Our results cannot exclude the possibility that at times during the Messinian Salinity Crisis, Mediterranean Outflow Water reached the Atlantic.

Keywords: Messinian Salinity Crisis, Mediterranean-Atlantic exchange, neodymium isotopes, Rifian Corridor, Mediterranean Outflow Water, Nd/Ca

1. Introduction

Before the formation of the Gibraltar Straits in the early Pliocene (e.g. Hsu, et al., 1973a, 1973b), two marine corridors linked the Mediterranean to the Atlantic; the Betic Corridor, in southern Spain, and the Rifian Corridor, in northern Morocco and Algeria (Fig. 1). Progressive restriction of these corridors is thought to have caused the Messinian Salinity Crisis (MSC), during which the Mediterranean underwent synchronous basin-wide, extreme salinity fluctuations (e.g. Hsu, et al., 1973b, 1977; Krijgsman et al., 1999a, 2002); at times becoming as much as ten-times as salty as the present day, while at others becoming almost fresh (Fig. 2).

Most of the hypotheses put forward to explain environmental fluctuations before, during and after the MSC relate to changes in Mediterranean-Atlantic exchange (Fig. 2). For several reasons, testing these hypotheses has proved challenging. First, the continental collision between Africa and Eurasia that closed the corridors (e.g. Krijgsman et al., 2004) also uplifted and eroded their sedimentary record. Consequently, no complete succession documenting the restriction and blocking of the corridors is preserved within them, and the timing of their closure is obscured by unconformities (Krijgsman, et al., 1999b; Hüsing et al., 2010). Second, reconstructing past exchange is difficult. Insights have been gained from studying faunal assemblages (e.g. Benson et al., 1991; Benammi et al., 1996; Carnevale et al., 2006) and sedimentary structures and facies (e.g. Cunningham and Collins, 2002; Betzler et al., 2006), while Sr isotopes have been used to monitor Mediterranean connectivity with the global ocean (Flecker et al., 2002; Topper et al., 2011). None of these datasets, however, provide a continuous record of exchange spanning the MSC, so testing the causal hypotheses for the different extreme environments has not been possible. In addition, this absence of a palaeo-record of Mediterranean-Atlantic exchange makes it impossible to evaluate the global influence of Mediterranean Outflow Water (MOW) during the MSC.

Today, MOW preconditions the intermediate-level North Atlantic with relatively warm, salty water (e.g. Boyer et al., 2009), which, as it spreads northwards and cools, is thought to contribute towards destabilising the high latitude water column and stimulating deep water formation (Mauritzen et al., 2001; McCartney and Mauritzen, 2001; New et al., 2001; Bower et al., 2002). Thus, past restricted exchange or cessation of MOW may have affected North Atlantic circulation and hence climate (e.g. Bigg and Wadley, 2001; Rogerson et al., 2010, 2012; Penaud et al., 2011) as could MOW with salinities significantly different from today (Ivanovic, 2012; Ivanovic et al., 2013). In addition, Messinian ocean circulation was likely to have been more susceptible to changes in MOW than the modern ocean, due to the presence of a weaker AMOC with respect to the present day; see Ivanovic et al. (2012) and references therein. Together with modelling experiments, a record of Mediterranean-Atlantic exchange would indicate whether the impact of the MSC was confined to the Mediterranean or had wider climatic influence.

Here, we present a new bottom water neodymium (Nd) isotope record reconstructed from late Miocene-Pliocene samples collected along the length of the Rifian Corridor. Seawater acquires its Nd isotopic signal through riverine and aeolian delivery of weathered continental crust (e.g. Goldstein and Jacobsen, 1987; Goldstein and Hemming, 2003; van de Flierdt et al., 2004) and exchange at the sediment water interface (boundary exchange; e.g. Lacan and Jeandel, 2005; Arsouze et al., 2007; Rempfer et al., 2011, 2012). Since the residence time of Nd is shorter than the global ocean mixing time (Broecker et al., 1960; Tachikawa et al., 1999, 2003; Arsouze et al., 2009) and because Nd isotopes are unaffected by water age, nutrient cycling or biological productivity (Martin and Haley, 2000; Frank, 2002; Goldstein and Hemming, 2003), oceanic water masses have distinct $^{143}Nd/^{144}Nd$ (expressed as $\varepsilon_{Nd} = [(^{143}Nd/^{144}Nd_{sample})/ (^{143}Nd/^{144}Nd_{CHUR}) -1] \times 10^4$, where CHUR is 0.512638, normalised to $^{146}Nd/^{144}Nd = 0.7219$; Jacobsen and Wasserburg, 1980) controlled by proximal average crustal Nd isotopic compositions and river catchment geology at the continental input source. For example, modern MOW is distinguishable from the Atlantic water into which it flows; -9.4 ε_{Nd} and -11.8 ε_{Nd} respectively (Fig. 1). This means that ε_{Nd} preserved in fossil marine substrate (including fish remains and foraminifera) can be used to trace seawater provenance over geological timescales. Previous studies (Abouchami et al., 1999; Muiños et al., 2008) measuring ε_{Nd} and lead isotopes in late Miocene eastern Atlantic ferromanganese (Fe-Mn) crusts show no sign that MOW was ever blocked during the MSC. However, these slow-growing archives (few mm Myr^{-1}) record a time-averaged signal that cannot resolve individual MSC events and a higher resolution record is required. Neodymium isotopic records from well preserved, calcareous benthic foraminifera and fish remains (bone fragments and teeth) have been shown to record and preserve bottom seawater ε_{Nd} reliably, often with resolution significantly higher than 10 ka (Staudigel et al., 1985; Martin and Haley, 2000; Thomas et al., 2003; Martin and Scher, 2004; Via and Thomas, 2006; Klevenz et al., 2008; Roberts et al., 2010; Scher and Delaney, 2010; Horikawa et al., 2011; Martin et al., 2012).

Here, we seek to reconstruct changes in Mediterranean-Atlantic water exchange during the late Miocene (8-5 Ma), spanning the period leading up to, during and immediately following the MSC. In particular, we aim to clarify the age at which the Rifian Corridor closed and test the hypothesis known as the Siphon Event (Fig. 2), which postulates that all Atlantic inflow to the Mediterranean was funnelled through the Rifian Corridor while outflow occurred exclusively through the Betic Corridor (Benson et al., 1991).

2. Methods

The palaeogeography of the Rifian Corridor is thought to have been complex (Fig. 1) and the flow pattern may therefore have been more similar to that observed in the Indonesian seaway today (e.g. Hautala et al., 2001; Potemra et al., 2003; Sprintall et al., 2009) than the simple, two-layer exchange that occurs through the Gibraltar Straits (e.g. Bethoux and Gentili, 1999; Tsimplis and Bryden, 2000). Sediment samples were obtained from two Deep Sea Drilling Project cores in the eastern North Atlantic (DSDP-14-135 and DSDP-79-547) as well as from boreholes and exposed successions situated along the now relict Rifian Corridor (Fig. 1; Supplementary Table S1). All the land sections have high resolution, astronomically-tuned age models, while lower resolution biostratigraphy is available for the DSDP cores (Fig. 3).

Sediments from the DSDP cores were deposited in open marine settings not dissimilar to the environments of their present day location (Hayes et al., 1972; Hinz et al., 1984). Five samples containing fish remains were analysed from these (Supplementary Table S2).

Four sections from the Bou Regreg Valley succession close to Morocco's Atlantic coast (Salé, Loulja A, Ain el Beida, Oued Akrech) span the entire period of interest (8.90-4.96 Ma; Figures 1 and 3). These sections comprise alternating indurated and less-well indurated marls (Fig. 3) typical of the Blue Marl Formation (Hodell et al., 1994; Hilgen et al., 2000; Krijgsman et al., 2004; van Assen et al., 2006; van der Laan et al., 2006). Palaeogeographic reconstructions suggest that these sections were located in the centre of a broad embayment, open to the Atlantic to the west and with the mouth of the Rifian Corridor to the east (Fig. 1). Like the Atlantic DSDP cores, the Bou Regreg Valley sections record continuous open marine sedimentation throughout, with none of the unconformities or extreme salinity fluctuations seen in coeval Mediterranean successions. Benthic foraminifera and fish remains were obtained from samples ranging in age from 7.39-5.15 Ma (Fig. 3; Supplementary Table S2).

The Zobzit section from the Taza-Guercif Basin is located in central northern Morocco, in the middle of the Rifian Corridor (Fig. 1). Palaeogeographic reconstructions (e.g. Fig. 1) suggest that it was located in one of the southern strands of the corridor's complex seaway.

The marine part of this section covers ~8.0-7.1 Ma and is dominated by marine marls and turbiditic sandstones (Fig. 3). Benthic/planktic foraminifera ratios indicate that the succession shallows upwards, culminating in an unconformity overlain by continental sediments equivalent in age to the MSC sequences (Krijgsman et al., 1999b). This has been interpreted to indicate the emergence of the Taza-Guercif Basin by 6.0 Ma, while closure of this strand of the corridor is thought to have occurred between 6.0-6.7 Ma (Krijgsman et al., 1999b). Samples containing both benthic foraminifera and fish remains were obtained from this section, ranging from 7.62-7.20 Ma (Supplementary Table S2).

The Messâdit section from the Melilla Basin on Morocco's Mediterranean coast at the eastern end of the Rifian Corridor (Fig. 1) spans 7.00-5.97 Ma (Fig. 3), recording conditions shortly before the first Mediterranean gypsum precipitated (Fig. 2). This succession is primarily composed of precession controlled blue-brown diatomaceous marl (rich in foraminifera, ostracods, fish remains and bivalves), intercalated with volcanic tuffs and ashes (Fig. 3) from the nearby Trois Fourges (acidic) and Gourougou (basic) volcanic centre (van Assen et al., 2006). The depositional environment is thought to have shallowed progressively culminating in a Halimeda packstone (Fig. 3), suggesting that the final stages of Messâdit deposition occurred in a very shallow lagoonal to lacustrine environment (van Assen et al., 2006). Fish remains were obtained from five samples ranging from 6.8-6.3 Ma.

2.1. Analytical techniques

The sample bulk sediments (>63 μm) were thoroughly washed in ultra-pure, filtered and deionised water and oven-dried at 60 °C. They were then hand-picked under a microscope to separate the >150 μm fish remains (teeth and bone fragments) and well preserved mixed species of calcareous benthic foraminifera (Supplementary Table S2); no attempt was made to distinguish between epifaunal and infaunal species as this should not affect the preserved

ε_{Nd} (Klevenz et al., 2008). Neodymium is incorporated into foraminiferal tests in relatively low concentrations, especially compared to the hydroxyfluorapatite of fish teeth and bones (e.g. Staudigel et al., 1985; Vance and Burton, 1999; Martin and Haley, 2000; Klevenz et al., 2008; Martínez-Botí et al., 2009). To yield sufficiently high Nd concentrations for a single ε_{Nd} measurement, target counts per sample were 600 (minimum 300) benthic foraminifera, and several fish tooth/bone fragments (minimum 1); actual counts are given in Supplementary Table S2.

After opening the individual foraminiferal test-chambers by careful crushing, procedural blanks were introduced. All samples (foraminifera and fish remains, including procedural blanks) underwent multiple rinses and ultrasonication in ultra-pure water and methanol to remove any adherent fine-grained particles. For consistency with previous work on foraminifera samples from the region (Ivanovic, 2012), the samples next underwent reductive and oxidative cleaning steps to remove ferromanganese coatings/organic material and measure only the calcite-bound Nd (Vance and Burton, 1999, modified from Boyle and Keigwin, 1985).

As a final cleaning step to remove any re-adsorbed Rare Earth Elements (REE), the samples were then rinsed in 1 mmol HNO_3. After this, a $^{149}Sm/^{150}Nd$ spike solution was added for isotope dilution measurements and an aliquot of each sample solution was separated and sealed ready for measuring the element/Ca ratios. Neodymium and Sm fractions have been purified using standard techniques (Cohen et al., 1988; Pin and Zalduegui, 1997).

All sample preparation and mass-spectrometric measurements were carried out in the Bristol Isotope Group within the Department of Earth Sciences, University of Bristol (UK). The element/Ca ratios were measured relative to a Bristol Spiked Gravimetric Standard (BSGS) over four analytical sessions (October 2010 to March 2012) using a Thermo

Finnigan Element 2 ICP-MS. These ratios have an estimated precision of better than 5 %. The Nd and Sm isotope compositions were measured over five analytical sessions (January 2010 to March 2012) in static mode on a Thermo-Finnigan Neptune MC-ICP-MS. For Nd measurements, correction of the instrument-induced mass bias followed Vance and Thirlwall [2002], adjusting to a $^{146}Nd/^{144}Nd$ of 0.7219. Mass-bias corrected ratios were subsequently normalised to the given $^{143}Nd/^{144}Nd$ of the La Jolla standard of 0.511856. The long-term external mass spectrometric reproducibility is better than 0.2 ε_{Nd} for Nd isotope measurements at ^{144}Nd ion currents of around 7×10^{-11} A (50 ppb Nd solutions), and 0.4 ε_{Nd} at ^{144}Nd ion currents of around 1.4×10^{-11} A (10 ppb Nd solutions). The total procedural Nd blank was 31-73 pg (n=5). This is equivalent to ~0.02-0.96 % (mean 0.26 %) and ~0.02-0.61 % (mean 0.24 %) of the total Nd measured in the fish remains and foraminifera samples respectively. Hence in all samples, the total procedural blank contribution is <1 % (mean <0.23 %) and so is insignificant (Supplementary Fig. S1). Samarium isotopic compositions have been mass bias corrected using a natural $^{147}Sm/^{149}Sm$ of 1.08507.

Sample $^{147}Sm/^{144}Nd$ ratios measured by isotope dilution have an external precision better than 0.5 %. All measured $^{143}Nd/^{144}Nd$, $^{147}Sm/^{144}Nd$ and ε_{Nd} values are given in Supplementary Table S3. The reported $\varepsilon_{Nd(T)}$ ratios have been corrected for post-depositional ^{143}Nd ingrowth using the equation of Faure and Mensing (2004).

3. Results

3.1 Primary/secondary origin of the $\varepsilon_{Nd(T)}$ signal

There is strong evidence that fish teeth and bones post-depositionally acquire their Nd in relatively high concentrations (>200 ppm) when they are still in contact with seawater, thus recording sediment porewater ε_{Nd} that is in equilibrium with bottom seawater ε_{Nd} (incl. Staudigel et al., 1985; Martin and Haley, 2000; Thomas et al., 2003; Martin and Scher, 2004;

Scher and Delaney, 2010; Horikawa et al., 2011). These studies also show that this primary ε_{Nd} is preserved in the fish remains over geologic timescales because (a) the initially acquired concentrations are so high and (b) Nd is relatively chemically inert during burial and lithification. However, questions remain over whether the same is true for foraminifera (e.g. Palmer and Elderfield, 1985, 1986; Sholkovitz, 1989; Pomiès et al., 2002; Vance et al., 2004; Klevenz et al., 2008; Martínez-Botí et al., 2009; Roberts et al., 2010, 2012). For example, Roberts et al. (2010) show that >90 % of the authigenic Fe-Mn oxyhydroxide foraminifera coatings must be removed to extract the pristine calcite-bound ε_{Nd}. Element/Ca ratios measured in benthic foraminiferal tests (Supplementary Table S4) can be used to ascertain whether the Nd isotope signal measured in foraminifera is controlled by foraminiferal calcite-derived Nd or Fe-Mn oxyhydroxide coatings. In the absence of direct late Miocene seawater measurements, these ratios are the best means of determining the efficacy of the cleaning protocol. Previous studies suggest that samples with Mn/Ca ratios >300-400 μmol mol^{-1} may have diagenetically-offset $\varepsilon_{Nd(T)}$, whereas below these values, contaminant Nd concentrations are probably too low to obscure the primary seawater ε_{Nd} (Vance and Burton, 1999; Burton and Vance, 2000; Vance et al., 2004). All data reported here have Mn/Ca ratios under 200 μmol mol^{-1}, with the majority under 100 μmol mol^{-1}.

The relationships between sample Nd/Ca and Mn/Ca, Nd/Ca and age, Mn/Ca and age, and Mn/Ca and $\varepsilon_{Nd(T)}$ were also examined (Fig. 4) to evaluate the likelihood of diagenetic overprinting. Contrary to previous work on sedimentary and plankton-towed foraminifera (Pomiès et al., 2002; Martínez-Botí et al., 2009), we find no strong relationship between Nd/Ca and Mn/Ca (Fig. 4a; correlation <0.25). Samples from the Zobzit section generally have higher Nd/Ca (>0.60 μmol mol^{-1}) and higher Mn/Ca (>130 μmol mol^{-1}) than samples from the more westerly Bou Regreg Valley sections in close proximity to the Atlantic. The higher element/Ca ratios of the Zobzit foraminiferal tests may indicate a higher concentration of REE in the water overlying Zobzit than in the water above the Bou Regreg Valley sections. This is perhaps unsurprising given the more continental palaeo-setting of Zobzit relative to the more oceanic environment of the Salé, Loulja A, Ain el Beida and Oued Akrech sections (Fig. 1). Zobzit's central position is likely to have resulted in greater fluvial and aeolian delivery of REE, leading to higher dissolved REE concentrations in local seawater (e.g. Jeandel et al., 1995; Rempfer et al., 2011; Lacan et al., 2012; Pahnke et al., 2012).

If Mn and Nd are acquired by foraminiferal tests through on-going diagenesis, then, assuming that the cleaning protocol is equally effective for all samples regardless of age, older samples could be relatively enriched in these REE. A visual comparison between Nd/Ca and age (Fig. 4b) and between Mn/Ca and age (Fig. 4c) indicates a tentative relationship, but the scatter is large and the correlations between sample age and both element/Ca ratios are not statistically significant (<0.18 and 0.30, respectively). When the data from different locations (Bou Regreg Valley versus Zobzit) are considered independently, the correlation coefficients degrade even further to <0.003 for Nd/Ca and age, and <0.045 for Mn/Ca and age, suggesting that diagenetic processes leave little imprint on the Nd measured in benthic foraminifera.

The correlation between Mn/Ca and $\varepsilon_{Nd(T)}$ (Fig. 4d) can also be used to check for secondary alteration of the primary bottom water signal in benthic foraminifera. For example, if Nd associated with diagenetic Fe-Mn coatings contaminates the original seawater ε_{Nd} then there should be a correlation between Mn/Ca and $\varepsilon_{Nd(T)}$. This is because Mn-enrichment in samples is an indication of exposure to authigenic and/or diagenetic sources of Nd (e.g. Vance and Burton, 1999; Pena et al., 2005, 2008; Martínez-Botí et al., 2009), which mainly reflect local geology and should be relatively constant through time. Thus, the diagenetic influence on samples would be to have high Mn/Ca and to trend towards an authigenic $\varepsilon_{Nd(T)}$

signal. Again, there is no correlation between Mn/Ca and $\varepsilon_{Nd(T)}$ (Fig. 4d) to suggest significant overprinting of the original seawater ε_{Nd}. In addition, recent studies of uncleaned planktic foraminifera show that, like fish remains, authigenic $\varepsilon_{Nd(T)}$ measured in Fe-Mn oxyhydroxide coatings is acquired at the ocean sediment-water interface, recording bottom water $\varepsilon_{Nd(T)}$ (Roberts et al., 2010, 2012; Piotrowski et al., 2012). Consequently, although we reductive-oxidatively cleaned our samples in an attempt to measure the calcitic Nd and thus extract the $\varepsilon_{Nd(T)}$ of bottom seawater during the foraminferas' lifecycle, any Nd from residual Fe-Mn oxhydroxide coatings should also reflect the same bottom water $\varepsilon_{Nd(T)}$.

The foraminiferal data shows a range of around 2.5 ε_{Nd} (Fig. 4d), which may be explained by temporal changes in corridor dynamics and circulation. This would affect the relative contributions from different seawater ε_{Nd} sources (e.g. Atlantic versus Mediterranean) as well as fluvial delivery and volcanic sources of ε_{Nd} (e.g. Palmer and Elderfield, 1985; Kocsis et al., 2009). The Zobzit samples have more radiogenic ε_{Nd} than almost all the Bou Regreg Valley samples; again this could reflect Zobzit's central position in the corridor, which is likely to have been less influenced by relatively unradiogenic Atlantic water ε_{Nd} and more influenced by local radiogenic sources of Nd.

Duplicate measurements were only possible for samples containing abundant fish remains or where the sample contained both fish material and abundant benthic foraminifera. Multiple analyses were carried out on ten samples. Of these, the results of eight were within error of each other (Fig. 5), giving confidence in the signal recorded. The two samples with results that are not within error were measured in concomitant fish remains and benthic foraminifera (Oued Akrech OAK-60.3, Zobzit MA-75; Supplementary Table S2). There is no evidence to suggest that any of these measurements reflect diagenetic or analytical errors. However, given that a single fish fragment is all that is required for Nd isotope analysis, sedimentary reworking or bioturbation of fish remains is a distinct possibility. The benthic foraminiferal measurements are made from the combined material of several hundred individuals specimens (802 for OAK-60. 3; 342 for MA-75) and hence are much less vulnerable to post-depositional disturbance. We conclude that where measurements from different archives in the same sample are disparate, both the data are genuine seawater ε_{Nd}, but were recorded at different times. In these instances, benthic foraminifera $\varepsilon_{Nd(T)}$ probably pertains to the age of sample sediment deposition, while fish remains $\varepsilon_{Nd(T)}$ could either be slightly younger due to bioturbation or slightly older through sediment reworking.

In summary, the data suggest that diagenetic Nd has not significantly overprinted the ε_{Nd} measured in these samples and thus, in light of previous evidence (incl. Vance and Burton, 1999; Burton and Vance, 2000; Vance et al., 2004; Klevenz et al., 2008; Martínez-Botí et al., 2009; Roberts et al., 2010, 2012; Elmore et al., 2011; Charbonnier et al., 2012; Piotrowski et al., 2012), we propose that the $\varepsilon_{Nd(T)}$ in both fish remains and benthic foraminifera archives reflect the $\varepsilon_{Nd(T)}$ of bottom seawater at their time of deposition.

3.2. Atlantic and Mediterranean end-member $\varepsilon_{Nd(T)}$

Constraints on the $\varepsilon_{Nd(T)}$ values for late Miocene Atlantic and Mediterranean water masses are required to reconstruct exchange through the Rifian Corridor. Ancient seawater $\varepsilon_{Nd(T)}$ can be obtained indirectly through the analysis of fossil archives (e.g. Staudigel et al., 1985; Vance and Burton, 1999; Martin and Haley, 2000; Frank, 2002; Goldstein and Hemming, 2003; Katz et al., 2010). In this study the local palaeo-Atlantic end-member $\varepsilon_{Nd(T)}$ is derived from late Miocene to early Pliocene fish remains from the Atlantic DSDP sites (Fig. 1). Three of the four DSDP samples give $\varepsilon_{Nd(T)}$ data that are within error of each other and are unradiogenic relative to most of the on-shore samples (Fig. 5; Supplementary Table S3). This suggests that the late Miocene Atlantic end-member $\varepsilon_{Nd(T)}$ was probably between -9.9 and -10.8 (Fig. 5); around 1.5 ε_{Nd} more radiogenic than nearby water measurements for the present day (Spivack and Wasserburg, 1988). There are various possible explanations for why the oldest fish tooth recorded a more radiogenic $\varepsilon_{Nd(T)}$ (Fig. 5). For example, the data may track an increased contribution of MOW to the eastern North Atlantic compatible with wider Rifian and Betic Corridors in the Tortonian. Alternatively, a change in eastern Atlantic water provenance (such as an increase in Southern Source Waters and/or a decrease in NADW) may have raised the ε_{Nd} over DSDP-14-135.

We have constrained the $\varepsilon_{Nd(T)}$ of Mediterranean water in the Rifian Corridor based on measurements from the lowest part of the Messâdit section, which is at the Mediterranean end of the corridor (Fig. 1). Detailed faunal and sedimentological analysis of this and other sections in the Melilla Basin indicate that the onset of cyclic sedimentation at the base of the section (6.84 Ma) is coincident with a basin-wide highstand (Saint Martin and Cornee, 1996; van Assen et al., 2006). At 6.72 Ma, a colour change in Messâdit sediments is coeval with a change in the benthic foraminiferal species that flourish in restricted waters (van Assen et al., 2006). This event correlates with the lower-to-upper Abad transition in the Betic Corridor (Sorbas Basin) and is thought to reflect increasing tectonic activity in the Betic-Rif zone (Martín and Braga, 1994; Sierro et al., 2001, 2003; van Assen et al., 2006). Therefore, $\varepsilon_{Nd(T)}$ derived from sediments younger than 6.72 Ma probably reflect a more local, restricted Melilla Basin subject to more pronounced boundary exchange, riverine and aeolian influences than those that predate this event. Consequently, our constraints on the most Mediterranean-like ε_{Nd} entering the corridor at its eastern end during the late Miocene are derived from fish remains sampled close to the base of the Messâdit section at 6.83 Ma. This provides a working approximation of the late Miocene western Mediterranean end-member $\varepsilon_{Nd(T)}$ (-8.2 to -8.9, Fig. 5) that is around 0.9 ε_{Nd} more radiogenic than nearby water measurements for the present day (Fig. 5.; Spivack and Wasserburg, 1988; Henry et al., 1994; Tachikawa et al., 2004). The difference may reflect evolution of western Mediterranean ε_{Nd}

from a dominantly (more radiogenic) Eurasian-Northeast African input during the Messinian to an increasing Northwest African (generally less radiogenic) influence today (Henry et al., 1994; Abouchami et al., 1999; Scrivner et al., 2004) and/or the influence of local, basic volcanism (van Assen et al., 2006). Messâdit seawater could also incorporate a component of eastward flowing Atlantic water, although at the easternmost end of the Rifian Corridor, any Atlantic influence is likely to have been relatively weak. This is borne out by the clear difference between reconstructed $\varepsilon_{Nd(T)}$ of the palaeo-Atlantic and palaeo-Mediterranean (Fig. 5). Moreover, both the Mediterranean and eastern North Atlantic Messinian $\varepsilon_{Nd(T)}$ end-members are more radiogenic than present-day ε_{Nd} and are consistent with previous palaeo-measurements in the region (e.g. Abouchami et al., 1999; Muiños et al., 2008).

3.3. Exchange evolution

Assuming these Atlantic and Mediterranean end-members are reasonable for late Miocene water entering the Rifian Corridor, they can be used to interpret the ε_{Nd} data from samples in terms of the relative contributions made by the two water masses. The temporal variability of data from each sample site (Fig. 5) is revealing and helps to test the various hypotheses for changing patterns of exchange.

The lower three samples from the Zobzit section (7.62-7.25 Ma) are relatively radiogenic and plot within error of estimated palaeo-Mediterranean values (Box A, Fig. 5). Data from the overlying sediments (7.22 and 7.20 Ma) are highly variable, showing first an excursion to less radiogenic $\varepsilon_{Nd(T)}$, including one within error of the palaeo-Atlantic end-member, followed by an extremely radiogenic sample (-1.60 $\varepsilon_{Nd(T)}$ ±0.35) at 7.20 Ma (Excursion B, Fig. 5). Benthic/planktic foraminiferal ratios indicate that this increase in variability coincides with rapid shallowing (5 m ka^{-1}) of the Taza-Guercif Basin (Krijgsman et al., 1999b). The shallowing has been attributed to a combination of glacio-eustatic sea level fall (~40 m;

Hodell et al., 1994) and an increased sedimentation rate associated with tectonic uplift (360 m; Krijgsman et al., 1999b). One possible explanation for the temporal evolution of Zobzit $\varepsilon_{Nd(T)}$ is that initial Taza-Guercif shallowing occurred to the east of the section, restricting exchange with the Mediterranean whilst maintaining a relatively good connection with the Atlantic. Subsequent rapid shallowing restricted exchange in both directions, leading to the dominance of locally derived, distinct seawater ε_{Nd} (through boundary exchange and/or fluvial and aeolian inputs), which caused the excursion to very radiogenic $\varepsilon_{Nd(T)}$ in the youngest Zobzit sample. A significant contribution of water draining local volcanic terrain (Fig. 1) could explain why the Nd isotope excursion is so extreme.

A trend towards more radiogenic $\varepsilon_{Nd(T)}$ is also observed in the Messâdit data (Box A, Fig. 5) with the youngest sample, taken <4 m below the first Halimeda packstone horizon, showing more radiogenic ε_{Nd} than the palaeo-Mediterranean end-member. Given the sedimentological evidence for shallowing and the intercalation of volcanic ash (van Assen et al., 2006), it seems likely that this $\varepsilon_{Nd(T)}$ trend also reflects a relative increase in the influence of locally derived Nd with time.

The $\varepsilon_{Nd(T)}$ record extracted from the Bou Regreg Valley samples spans the entire MSC period (7.39-5.15 Ma). Three distinct distributions can be seen in these data (Fig. 5):

Box A. The oldest samples plot within error of palaeo-Atlantic end-member values. These are overlain by samples showing a trend towards more radiogenic $\varepsilon_{Nd(T)}$, including some within error of the estimated palaeo-Mediterranean end-member $\varepsilon_{Nd(T)}$. The onset of this trend is coeval with the extreme variability seen at Zobzit (7.20-7.25 Ma) and the measurement at 6.64 Ma is within error of both palaeo-Mediterranean and Messâdit ε_{Nd} of roughly the same age. The transition from palaeo-Atlantic-like water $\varepsilon_{Nd(T)}$ to palaeo-Mediterranean-like water $\varepsilon_{Nd(T)}$ indicates the increasing influence of more radiogenic water at the western end of the Rifian Corridor 7.2-6.6 Ma. A possible source of this radiogenic water is westward flow through the corridor from the Mediterranean. Such flow may be modified by boundary exchange with radiogenic sediments flooring the corridor (e.g. in the Taza-Guercif and Melilla Basins; Figures 1 and 5), in a similar manner to the ‘renewal’ of Pacific water as it passes over the Java Shelf today (Jeandel et al., 1998; Lacan and Jeandel, 2005).

Box C. Between 6.5 and 5.9 Ma in the Bou Regreg Valley sections, $\varepsilon_{Nd(T)}$ are consistently around -9.5, plotting between the estimates of palaeo-Atlantic and -Mediterranean seawater. These samples are rather less radiogenic than the youngest Bou Regreg Valley sample in Box A, suggesting a shift back towards more Atlantic-influenced water at the western end of the corridor 6.64-6.44 Ma.

Box D. The youngest samples from the Bou Regreg Valley sections, generally have more radiogenic $\varepsilon_{Nd(T)}$ than those in Box C, varying from within error of palaeo-Mediterranean water to less radiogenic values around -9.2. This shift suggests reduced Atlantic-water influence from ~5.8 Ma onwards. The variability in $\varepsilon_{Nd(T)}$ during the MSC is quite large and there are hints that the record shows periodic fluctuations which may correlate with specific MSC events.

Notably, from 7.1 Ma onwards, Bou Regreg foraminifera and fish debris $\varepsilon_{Nd(T)}$ are 1-4 $\varepsilon_{Nd(T)}$ more radiogenic than nearby Atlantic sediments, despite the close proximity of these two localities (Figures 1 and 5). The variability in the youngest data (Box D, Fig. 5) and disparity with local seafloor $\varepsilon_{Nd(T)}$ (Fig. 1) strongly suggests that the archives record changes in water provenance (i.e. relatively radiogenic MOW and continental drainage) rather than being dominated by exchange with seafloor sediments. To test this conclusion, future work will examine the samples’ detrital fraction.

4. Discussion and hypothesis testing

4.1. Siphon Event

Faunal analysis of the Bou Regreg Valley sections by Benson et al. (1991) identified a shift in the ostracod assemblage at the Tortonian-Messinian boundary (~7.2 Ma) where warm shallow water species were abruptly replaced by colder, deeper dwelling types typically found in the Atlantic. This led the authors to suggest that between 6.4 and 5.3 Ma (later revised to 7.20 and 6.58 Ma; incl. van Assen et al., 2006), Atlantic water was siphoned into the Mediterranean only through the Rifian Corridor, while all MOW flowed out through the Betic Corridor. Subsequently stable isotope analysis of the Salé Section showed an increase in benthic foraminifera $\delta^{18}O$ over the Tortonian-Messinian boundary; attributed to cooling and/or increasing salinity of Rifian Corridor seawater, and linked to the siphon circulatory hypothesis (Hodell et al., 1994, 2001). Changing carbonate facies in the coeval Melilla Basin (Fig. 1) has also been attributed to the flow of cooler, nutrient-rich waters (Cunningham and Collins, 2002) thought to be of Atlantic origin (Esteban, 1979; Cunningham and Collins, 2002). In addition, later changes in faunal and sedimentary facies and their associated temperature changes have been linked to the termination of the siphon event (Cunningham and Collins, 2002; van Assen et al., 2006). This includes the onset of white, mm-laminated diatomite deposition in the Melilla Basin, a change from boreal to tropical diatom species (van Assen et al., 2006) and the onset of prograding Porites fringing reefs (Roger et al., 2000), which all occurred at 6.58 Ma.

This new record of Bou Regreg Valley bottom water $\varepsilon_{Nd(T)}$ allows us to test the hypothesis that Atlantic water was siphoned through the Rifian Corridor in the early Messinian. Today, the Mediterranean's freshwater deficit (0.04-0.11 Sv; caused by high evaporation) draws ~0.7-0.8 Sv of Atlantic water into the Mediterranean (Bryden et al., 1994; Tsimplis and Bryden, 2000; Dubois et al., 2011). However, recent general circulation modelling suggests that the Messinian Mediterranean-Atlantic density gradient was even greater (Ivanovic, 2012). This, and the much wider geometry of the Rifian and Betic corridors compared to the Gibraltar Straits (Fig. 1), suggests that Messinian Atlantic inflow was at least as strong, if not stronger, than at present. Thus, if the siphon event did occur, $\varepsilon_{Nd(T)}$ within error of palaeo-Atlantic constraints should be observed in the Rifian Corridor at this time. In fact, the Nd record shows something different; samples older than 7.2 Ma are largely within error of palaeo-Atlantic water, but those falling during the proposed siphoning period have more radiogenic values, some even within error of Mediterranean $\varepsilon_{Nd(T)}$ (Fig. 5, Box A). Our data are therefore consistent with a change in water mass affecting the Rifian Corridor at 7.2 Ma, but not with that water mass being exclusively Atlantic in origin. On the contrary, bottom water at the western end of the Rifian Corridor seems to have had an increasingly radiogenic influence, possibly from Mediterranean water that has been modified in the Rifian Corridor. Consequently it seems likely that the pattern of Mediterranean-Atlantic exchange described by the siphon hypothesis is not correct.

4.2. Timing of Rifian Corridor closure

There are various constraints on the timing of Rifian Corridor closure. Evidence of mammal exchange between Africa and Europe, (Benammi et al., 1996), places it before 6.1 Ma. Sedimentology and astronomical-tuning of Melilla Basin sections suggests that flow through the Rifian Corridor was restricted after 6.84 Ma, reduced to a minimum at 6.58 and terminated by 6.0 Ma (van Assen et al., 2006). Similar tuning of Taza-Guercif Basin sections led Krijgsman et al. (1999b) to constrain closure of the southern central part of the Corridor to 6.7-6.0 Ma. These relatively loose time constraints result largely from an unconformity, which is the product of the uplift and erosion associated with closure.

Located on specific strands of the complex Rifian seaway (Fig. 1), neither the Melilla nor Taza-Guercif studies can exclude the possibility that exchange persisted elsewhere in the corridor after it ceased in those specific areas. However, the Bou Regreg Valley sections in the bay west of the mouth of the corridor are well placed to monitor the entirety of Atlantic-Mediterranean exchange through the corridor. The only time that Bou Regreg Valley $\varepsilon_{Nd(T)}$ is within error of palaeo-Atlantic values is the earliest part of the section, ~7.15-7.40 Ma (Fig. 5). Even after the Gibraltar Straits open at 5.33 Ma, when only a single conduit for Mediterranean-Atlantic exchange existed, $\varepsilon_{Nd(T)}$ in the Loulja samples is much more radiogenic than this and is within error of palaeo-Mediterranean end-members (Fig. 5). Planktic/benthic ratios indicate that the western end of the corridor shallowed from 600-1000 m in the late Miocene (Ain el Beida Section; Benson and Rakic-El Bied, 1996; van der Laan et al., 2006) to 300-500 m in the latest Messinian/early Pliocene (van der Laan et al., 2006). This was probably caused by ongoing tectonic uplift, ultimately leading to the exposure of these marine sediments above sea level, several kilometres in-land. Consequently, the Bou Regreg Valley sections became more proximal to the coastline, increasing the influence of river run-off and aeolian input from the adjacent Moroccan land surface on local seawater ε_{Nd}. Hence, after the opening of the Gibraltar Straits, the relatively radiogenic $\varepsilon_{Nd(T)}$ recorded in the Pliocene marine sediments from the Bou Regreg Valley sections (Fig. 5) probably reflects a mixture of Atlantic water, fluvial/aeolian and margin-sediment Nd, and possibly some component of MOW from the north. At the same time, the data could be affected by changes in larger-scale ocean circulation and the varying depth of the water column resulting in different water masses being sampled at these sites.

In the early Pliocene, river run-off ε_{Nd} (which reflects the catchment hydrology) would have been dominated by the rocks flanking the corridor and earlier sediments deposited within the corridor itself as it was exposed, uplifted and eroded. Today, the major rivers in this area lie along the corridor axis. Thus, $\varepsilon_{Nd(T)}$ from the Mellila and Taza-Guercif Basins provide tentative constraints on the likely ε_{Nd} delivered by the westward-flowing rivers. The bottom seawater archives suggest that water at these locations was probably within error of palaeo-Mediterranean values (Fig. 5). However, the extremely radiogenic data recorded at Zobzit (Excursion B; Fig. 5) and measured in nearby volcanic complexes (Fig. 1) suggests that at times, corridor flank geology and exposed corridor sediments could have resulted in run-off that was more radiogenic than palaeo-Mediterranean values. Consequently, MOW is not required to explain Pliocene Bou Regreg seawater within error of palaeo-Mediterranean ε_{Nd}; it could have been generated by varying radiogenic riverine ε_{Nd}.

The increasing proximity of the Bou Regreg sections to the emerging coastline after the Tortonian could also explain why Bou Regreg $\varepsilon_{Nd(T)}$ does not fall within error of the palaeo-Atlantic signal after 7.2 Ma. This change away from Atlantic end-member composition is unlikely to have been a smooth, consistent transition, but rather a series of abrupt shifts reflecting the timing of tectonic events that restricted, closed and uplifted the corridor. One such shift occurs between 6.64 and 6.44 Ma; samples with $\varepsilon_{Nd(T)}$ within error of palaeo-Mediterranean water (Box A; Fig. 5) are overlain by less radiogenic values closer to palaeo-Atlantic estimates (Box C; Fig. 5). Irrespective of whether the end-member ε_{Nd} entering the western end of the corridor was a pure or dilute Atlantic signal, this shift away from palaeo-Mediterranean values indicates a significant decline in the influence of Mediterranean-like water. One likely explanation for this is partial or total blocking of Mediterranean-Atlantic exchange and the timing of the shift is consistent with previous estimates of Rifian closure (Benammi et al., 1996; Krijgsman, et al., 1999b; van Assen et al., 2006; Fig. 5). If the shift does represent corridor closure, it provides rather tighter constraints (6.64-6.44 Ma) on the event than previous estimates.

4.3 Mediterranean-Atlantic exchange during the MSC

It is difficult to explain the thick gypsum and halite precipitates observed across the Mediterranean without the supply of salty Atlantic water (e.g. Ryan et al., 1973; Cita et al., 1978). If Mediterranean-Atlantic connectivity prevailed, MOW may also have periodically reached the Atlantic, at least during the gypsum and brackish salinity events or at the beginning and end of Mediterranean hyper-/hypo-salinity (e.g. Flecker et al., 2002; Gladstone et al., 2007; Murphy et al., 2009; Meijer, 2012).

The $\varepsilon_{Nd(T)}$ record of the Bou Regreg Valley sections during the MSC is characterised by variability within error of, or slightly less radiogenic than palaeo-Mediterranean water (Box D; Fig. 5). We therefore need to consider the possible mechanisms for generating Mediterranean-like radiogenic $\varepsilon_{Nd(T)}$ after closure of the Rifian corridor. These include:

(i) Rivers draining rocks with relatively high ε_{Nd} (e.g. Fig. 1 and van Assen et al., 2006) supplying more radiogenic ε_{Nd} to the Bou Regreg Valley area; on-going tectonic uplift would change the drainage basin configuration and thus cause shifts in the fluvial ε_{Nd}.

(ii) Regional fluctuations in humidity, precipitation and wind patterns affecting the relative contribution of continental Nd inputs; mostly fluvial, but possibly some aeolian processes (e.g. Stumpf et al., 2011).

(iii) Changes in the volume, flow-rate and composition of MOW reaching the Bou Regreg Valley area through other Atlantic-Mediterranean connections e.g. the Gibraltar Straits.

Mechanisms (i) and (ii) are relatively straightforward, but (iii) requires more thought:

MOW derived contourites in the Gulf of Cadiz (Hernández-Molina et al., 2011) indicate that MOW contributed to eastern Atlantic bottom water after the Gibraltar Straits opened at 5.33 Ma. MOW's influence over the North Moroccan continental shelf area is unclear and cannot be excluded on the basis of the $\varepsilon_{Nd(T)}$ record presented here, since if MOW reached the

Pliocene Bou Regreg Valley, sample $\varepsilon_{Nd(T)}$ within error of the palaeo-Mediterranean range would be partly attributable to MOW input. Were this the case, earlier values within error of palaeo-Mediterranean estimates (e.g. Loulja A and Ain el Beida samples, Box D, Fig. 5) could plausibly represent MOW that was at least episodically present in the eastern North Atlantic during Mediterranean gypsum formation and Lago Mare (brackish water) conditions.

5. Conclusions

Neodymium isotopes from benthic foraminifera and fish remains provide the first bottom-seawater record of Rifian Mediterranean-Atlantic exchange spanning the MSC (8-5 Ma). The resulting record of flow through the Rifian Corridor suggests the hydrographic situation changed at 7.2 Ma, but prevailing water was not exclusively sourced from the Atlantic as required by the siphon hypothesis (7.20-6.58 Ma). Mediterranean water appears to have reached the western end of the corridor until ~6.64 Ma. However, the record suggests that the corridor shut between 6.64-6.44 Ma; well before the onset of the MSC. MOW-like ε_{Nd} is found at the western end of the corridor during and after the MSC. This may result from either the direct influence of MOW reaching the Atlantic elsewhere or as a consequence of local continental (mainly fluvial) inputs of radiogenic ε_{Nd}.

Acknowledgements

This work was funded by the University of Bristol Centenary Scholarship, Phyllis Mary Morris Fund and Daniel Pidgeon Fund. We are grateful to Frits Hilgen (Dept. Earth Sciences, Universiteit Utrecht, Netherlands), David Hodell (Dept. Earth Sciences, University of Cambridge, UK) and the curators of the IODP Bremen Core Repository (Germany) for kindly providing samples. We are also indebted to Nadia Barhoun (Université Hassan II – Mohammedia, Casablanca, Morocco) and Mohamed Zakaria Yousfi (Office National des

Hydrocarbures et des Mines, Rabat, Morocco) for invaluable field assistance as well as to Tanja Kouvenhoven for helpful discussions on the data. The continuous support of Chris Coath in keeping the Bristol Isotope Group clean lab. and mass spectrometric facilities working is greatly acknowledged and we thank Derek Vance for granting access to his labs and for constructive advice and discussions throughout the project. We are grateful to two anonymous reviewers for their valuable comments on the manuscript, and to Jean Lynch-Stieglitz for swift editorial handling.

References

Abouchami, W., Galer, S.J.., Koschinsky, A., 1999. Pb and Nd isotopes in NE Atlantic Fe–Mn crusts: Proxies for trace metal paleosources and paleocean circulation. Geochimica et Cosmochimica Acta 63, 1489–1505.

Ajaji, T., Weis, D., Giret, A., Bouabdellah, M., 1998. Coeval potassic and sodic calc-alkaline series in the post-collisional Hercynian Tanncherfi intrusive complex, northeastern Morocco: geochemical, isotopic and geochronological evidence. Lithos 45, 371–393.

Arsouze, T., Dutay, J.-C., Lacan, F., Jeandel, C., 2007. Modeling the neodymium isotopic composition with a global ocean circulation model. Chemical Geology 239, 165–177.

Arsouze, T., Dutay, J.-C., Lacan, F., Jeandel, C., 2009. Reconstructing the Nd oceanic cycle using a coupled dynamical – biogeochemical model. Biogeosciences 6, 2829–2846.

Benammi, M., Calvo, M., Prévot, M., Jaeger, J.-J., 1996. Magnetostratigraphy and paleontology of Aït Kandoula basin (High Atlas, Morocco) and the African-European late Miocene terrestrial fauna exchanges. Earth and Planetary Science Letters 145, 15–29.

Benson, R.H., Bied, K.R.-E., Bonaduce, G., 1991. An important current reversal (influx) in the Rifian Corridor (Morocco) at the Tortonian-Messinian boundary: The end of Tethys Ocean. Paleoceanography 6, P. 165.

Benson, R.H., Rakic-El Bied, K., 1996. The Bou Regreg section, Morocco: Proposed Global Boundary Stratotype Section and Point of the Pliocene. Notes et Mémoires du Service géologique, Maroc 383, 51–150.

Bethoux, J.P., Gentili, B., 1999. Functioning of the Mediterranean Sea: past and present changes related to freshwater input and climate changes. Journal of Marine Systems 20, 33–47.

Betzler, C., Braga, J.C., Martín, J.M., Sánchez-Almazo, I.M., Lindhorst, S., 2006. Closure of a seaway: stratigraphic record and facies (Guadix basin, Southern Spain). Int J Earth Sci (Geol Rundsch) 95, 903–910.

Bigg, G.R., Wadley, M.R., 2001. Millennial-scale variability in the oceans: an ocean modelling view. Journal of Quaternary Science 16, 309–319.

Bower, A.S., Le Cann, B., Rossby, T., Zenk, W., Gould, J., Speer, K., Richardson, P.L., Prater, M.D., Zhang, H.-M., 2002. Directly measured mid-depth circulation in the northeastern North Atlantic Ocean. Nature 419, 603–607.

Boyer, T.P., Antonov, J.I., Baranova, O.K., Garcia, H.E., Johnson, D.R., Locarnini, R.A., Mishonov, A.V., O'Brien, T.D., Seidov, D., Smolyar, I.V., Zweng, M.M., 2009. World Ocean Database 2009.

Boyle, E.A., Keigwin, L.D., 1985. Comparison of Atlantic and Pacific paleochemical records for the last 215,000 years: changes in deep ocean circulation and chemical inventories. Earth and Planetary Science Letters 76, 135–150.

Broecker, W.S., Gerard, R., Ewing, M., Heezen, B.C., 1960. Natural Radiocarbon in the Atlantic Ocean. J. Geophys. Res. 65, PP. 2903–2931.

Bryden, H.L., Candela, J., Kinder, T.H., 1994. Exchange through the Strait of Gibraltar. Progress in Oceanography 33, 201–248.

Burton, K.W., Vance, D., 2000. Glacial–interglacial variations in the neodymium isotope composition of seawater in the Bay of Bengal recorded by planktonic foraminifera. Earth and Planetary Science Letters 176, 425–441.

Carnevale, G., Landini, W., Sarti, G., 2006. Mare Versus Lago-Mare: Marine Fishes and the Mediterranean Environment at the End of the Messinian Salinity Crisis. Journal of the Geological Society 163, 75–80.

Charbonnier, G., Pucéat, E., Bayon, G., Desmares, D., Dera, G., Durlet, C., Deconinck, J.-F., Amédro, F., Gourlan, A.T., Pellenard, P., Bomou, B., 2012. Reconstruction of the Nd isotope composition of seawater on epicontinental seas: Testing the potential of Fe–Mn oxyhydroxide coatings on foraminifera tests for deep-time investigations. Geochimica et Cosmochimica Acta 99, 39–56.

Cita, M.B., Wright, R.C., Ryan, W.B.F., Longinelli, A., 1978. Messinian Paleoenvironments, in: Initial Reports of the Deep Sea Drilling Project, 42 Pt. 1 (Hsu Et Al., Eds). U.S. Government Printing Office.

Cohen, A.S., O'Nions, R.K., Siegenthaler, R., Griffin, W.L., 1988. Chronology of the pressure-temperature history recorded by a granulite terrain. Contributions to Mineralogy and Petrology 98, 303–311.

Cunningham, K.J., Collins, L.S., 2002. Controls on facies and sequence stratigraphy of an upper Miocene carbonate ramp and platform, Melilla basin, NE Morocco. United States Geological Survey.

Dubois, C., Somot, S., Calmanti, S., Carillo, A., Déqué, M., Dell'Aquilla, A., Elizalde, A., Gualdi, S., Jacob, D., L'Hévéder, B., Li, L., Oddo, P., Sannino, G., Scoccimarro, E., Sevault, F., 2011. Future projections of the surface heat and water budgets of the

Mediterranean Sea in an ensemble of coupled atmosphere–ocean regional climate models. Climate Dynamics.

Elmore, A.C., Piotrowski, A.M., Wright, J.D., Scrivner, A.E., 2011. Testing the extraction of past seawater Nd isotopic composition from North Atlantic deep sea sediments and foraminifera. Geochem. Geophys. Geosyst. 12, 13 PP.

Esteban, M., 1979. Significance of the upper miocene coral reefs of the Western Mediterranean. Palaeogeography, Palaeoclimatology, Palaeoecology 29, 169–188.

Flecker, R., de Villiers, S., Ellam, R.., 2002. Modelling the effect of evaporation on the salinity–87Sr/86Sr relationship in modern and ancient marginal-marine systems: the Mediterranean Messinian Salinity Crisis. Earth and Planetary Science Letters 203, 221–233.

Flecker, R., Ellam, R.M., 2006. Identifying Late Miocene episodes of connection and isolation in the Mediterranean-Paratethyan realm using Sr isotopes. Sedimentary Geology 188-189, 189–203.

Frank, M., 2002. Radiogenic isotopes: Tracers of past ocean circulation and erosional input. Rev. Geophys. 40, 38 PP.

Gladstone, R., Flecker, R., Valdes, P., Lunt, D., Markwick, P., 2007. The Mediterranean hydrologic budget from a Late Miocene global climate simulation. Palaeogeography, Palaeoclimatology, Palaeoecology 251, 254–267.

Goldstein, S.J., Jacobsen, S.B., 1987. The Nd and Sr isotopic systematics of river-water dissolved material: Implications for the sources of Nd and Sr in seawater. Chemical Geology: Isotope Geoscience section 66, 245–272.

Goldstein, S.L., Hemming, S.R., 2003. Long-lived Isotopic Tracers in Oceanography, Paleoceanography, and Ice-sheet Dynamics, in: Treatise on Geochemistry. H. D. Holland and K.l K. Turekian (eds), Pp. 625. Elsevier, pp. 453–489.

Gómez, F., 2003. The role of the exchanges through the Strait of Gibraltar on the budget of elements in the Western Mediterranean Sea: consequences of human-induced modifications. Marine Pollution Bulletin 46, 685–694.

Gradstein, F.M., Ogg, J.G., Smith, A.G., 2005. A Geologic Time Scale 2004. Cambridge University Press, Cambridge, UK.

Grousset, F.E., Biscaye, P.E., Zindler, A., Prospero, J., Chester, R., 1988. Neodymium isotopes as tracers in marine sediments and aerosols: North Atlantic. Earth and Planetary Science Letters 87, 367–378.

Grousset, F.E., Parra, M., Bory, A., Martinez, P., Betrand, P., Shimmield, G., Ellam, R.M., 1998. Saharan wind regimes traced by the Sr-Nd isotopic composition of subtropical Atlantic sediments: Last Glacial Maximum vs today. Quaternary Science Reviews 17, 395–409.

Hautala, S.L., Sprintall, J., Potemra, J.T., Chong, J.C., Pandoe, W., Bray, N., Ilahude, A.G., 2001. Velocity structure and transport of the Indonesian Throughflow in the major straits restricting flow into the Indian Ocean. J. Geophys. Res. 106, PP. 19,527–19,546.

Hayes, D.E., Pimm, A.C., et al., Hayes, D.E., Pimm, A.C., et al., 1972. Initial Reports of the Deep Sea Drilling Project, 14. U.S. Government Printing Office.

Henry, F., Jeandel, C., Dupré, B., Minster, J.-F., 1994. Particulate and dissolved Nd in the western Mediterranean Sea: Sources, fate and budget. Marine Chemistry 45, 283–305.

Hilgen, F.., Bissoli, L., Iaccarino, S., Krijgsman, W., Meijer, R., Negri, A., Villa, G., 2000. Integrated stratigraphy and astrochronology of the Messinian GSSP at Oued Akrech (Atlantic Morocco). Earth and Planetary Science Letters 182, 237–251.

Hilgen, F.J., Krijgsman, W., Langereis, C.G., Lourens, L.J., Santarelli, A., Zachariasse, W.J., 1995. Extending the astronomical (polarity) time scale into the Miocene. Earth and Planetary Science Letters 136, 495–510.

Hinz, K., Winterer, E.L., et al., Hinz, K., Winterer, E.L., et al., 1984. Initial Reports of the Deep Sea Drilling Project, 79. U.S. Government Printing Office.

Hodell, D.A., Benson, R.H., Kent, D.V., Boersma, A., Bied, K.R.-E., 1994. Magnetostratigraphic, biostratigraphic, and stable isotope stratigraphy of an Upper Miocene drill core from the Salé Briqueterie (northwestern Morocco): A high-resolution chronology for the Messinian stage. Paleoceanography 9, PP. 835–855.

Hodell, D.A., Curtis, J.H., Sierro, F.J., Raymo, M.E., 2001. Correlation of Late Miocene to Early Pliocene sequences between the Mediterranean and North Atlantic. Paleoceanography 16, 164–178.

Horikawa, K., Martin, E.E., Asahara, Y., Sagawa, T., 2011. Limits on conservative behavior of Nd isotopes in seawater assessed from analysis of fish teeth from Pacific core tops. Earth and Planetary Science Letters 310, 119–130.

Hsu, K.J., Cita, M.B., Ryan, W.B.F., 1973. The origin of the Mediterranean evaporite, in: Initial Reports of the Deep Sea Drilling Project, Eds. Ryan W. B. F. and Hsu, K. J. U.S. Government Printing Office, Washington D. C., pp. 1203–1231.

Hsu, K.J., Montadert, L., Bernoulli, D., Cita, M.B., Erickson, A., Garrison, R.E., Kidd, R.B., Mèlierés, F., Müller, C., Wright, R., 1977. History of the Mediterranean salinity crisis. Nature 267, 399–403.

Hsu, K.J., Ryan, W.B.F., Cita, M.B., 1973. Late Miocene Desiccation of the Mediterranean. Nature 242, 240–244.

Hüsing, S.K., Oms, O., Agustí, J., Garcés, M., Kouwenhoven, T.J., Krijgsman, W., Zachariasse, W.-J., 2010. On the late Miocene closure of the Mediterranean–Atlantic gateway through the Guadix basin (southern Spain). Palaeogeography, Palaeoclimatology, Palaeoecology 291, 167–179.

Ivanovic, R.F., 2012. Did Mediterranean Outflow Water affect global climate during the Messinian? Thesis, (PhD) University of Bristol, UK.

Ivanovic, R.F., Valdes, P.J., Flecker, R., Gutjahr, M., (2013) Sensitivity of modern climate to the presence, strength and salinity of Mediterranean-Atlantic exchange in a global General Circulation Model. Climate Dynamics. Available Online First. doi:10.1007/s00382-013-1680-5.

Jacobsen, S.B., Wasserburg, G.J., 1980. Sm-Nd isotopic evolution of chondrites. Earth and Planetary Science Letters 50, 139–155.

Jeandel, C., Bishop, J.K., Zindler, A., 1995. Exchange of neodymium and its isotopes between seawater and small and large particles in the Sargasso Sea. Geochimica et Cosmochimica Acta 59, 535–547.

Jeandel, C., Thouron, D., Fieux, M., 1998. Concentrations and isotopic compositions of neodymium in the eastern Indian Ocean and Indonesian straits. Geochimica et Cosmochimica Acta 62, 2597–2607.

Katz, M.E., Cramer, B.S., Franzese, A., Honisch, B., Miller, K.G., Rosenthal, Y., Wright, J.D., 2010. Tradtional and emerging geochemical proxies in foraminifera. Journal of Foraminiferal Research 40, 165–192.

Klevenz, V., Vance, D., Schmidt, D.N., Mezger, K., 2008. Neodymium isotopes in benthic foraminifera: Core-top systematics and a down-core record from the Neogene south Atlantic. Earth and Planetary Science Letters 265, 571–587.

Kocsis, L., Vennemann, T.W., Hegner, E., Fontignie, D., Tütken, T., 2009. Constraints on Miocene oceanography and climate in the Western and Central Paratethys: O-, Sr-, and Nd-isotope compositions of marine fish and mammal remains. Palaeogeography, Palaeoclimatology, Palaeoecology 271, 117–129.

Krijgsman, W., Blanc-Valleron, M.-M., Flecker, R., Hilgen, F.J., Kouwenhoven, T.J., Merle, D., Orszag-Sperber, F., Rouchy, J.-M., 2002. The onset of the Messinian salinity crisis in the Eastern Mediterranean (Pissouri Basin, Cyprus). Earth and Planetary Science Letters 194, 299–310.

Krijgsman, W., Gaboardi, S., Hilgen, F. j., Iaccarino, S., Kaenel, E. de, Laan, E. van der, 2004. Revised astrochronology for the Ain el Beida section (Atlantic Morocco): No glacio-eustatic control for the onset of the Messinian Salinity Crisis. Stratigraphy 1, 87–101.

Krijgsman, W., Hilgen, F.J., Raffi, I., Sierro, F.J., Wilson, D.S., 1999. Chronology, causes and progression of the Messinian salinity crisis. Nature 400, 652–655.

Krijgsman, W., Langereis, C.., Zachariasse, W.., Boccaletti, M., Moratti, G., Gelati, R., Iaccarino, S., Papani, G., Villa, G., 1999. Late Neogene evolution of the Taza–Guercif Basin (Rifian Corridor, Morocco) and implications for the Messinian salinity crisis. Marine Geology 153, 147–160.

Krijgsman, W., Meijer, P.T., 2008. Depositional environments of the Mediterranean “Lower Evaporites” of the Messinian salinity crisis: Constraints from quantitative analyses. Marine Geology 253, 73–81.

Lacan, F., Jeandel, C., 2005. Neodymium isotopes as a new tool for quantifying exchange fluxes at the continent-ocean interface. Earth and Planetary Science Letters 232, 245–257.

Lacan, F., Tachikawa, K., Jeandel, C., 2012. Neodymium isotopic composition of the oceans: A compilation of seawater data. Chemical Geology 300–301, 177–184.

Martin, E.E., Haley, B.A., 2000. Fossil fish teeth as proxies for seawater Sr and Nd isotopes. Geochimica et Cosmochimica Acta 64, 835–847.

Martin, E.E., MacLeod, K.G., Jiménez Berrocoso, A., Bourbon, E., 2012. Water mass circulation on Demerara Rise during the Late Cretaceous based on Nd isotopes. Earth and Planetary Science Letters 327–328, 111–120.

Martin, E.E., Scher, H.D., 2004. Preservation of seawater Sr and Nd isotopes in fossil fish teeth: bad news and good news. Earth and Planetary Science Letters 220, 25–39.

Martín, J., Braga, J.C., 1994. Messinian events in the Sorbas Basin in southeastern Spain and their implications in the recent history of the Mediterranean. Sedimentary Geology 90, 257–268.

Martin, J.M., Braga, J.C., Betzler, C., 2001. The Messinian Guadalhorce corridor: the last northern, Atlantic-Mediterranean gateway. Terra Nova 13, 418–424.

Martínez-Botí, M.A., Vance, D., Mortyn, P.G., 2009. Nd/Ca ratios in plankton-towed and core top foraminifera: Confirmation of the water column acquisition of Nd. Geochem. Geophys. Geosyst. 10, 16 PP.

Mauritzen, C., Morel, Y., Paillet, J., 2001. On the influence of Mediterranean Water on the Central Waters of the North Atlantic Ocean. Deep Sea Research Part I: Oceanographic Research Papers 48, 347–381.

McCartney, M.S., Mauritzen, C., 2001. On the origin of the warm inflow to the Nordic Seas. Progress in Oceanography 51, 125–214.

Meijer, P.T., 2012. Hydraulic theory of sea straits applied to the onset of the Messinian Salinity Crisis. Marine Geology 326–328, 131–139.

Muiños, S.B., Frank, M., Maden, C., Hein, J.R., Flierdt, T. van de, Lebreiro, S.M., Gaspar, L., Monteiro, J.H., Halliday, A.N., 2008. New constraints on the Pb and Nd isotopic evolution of NE Atlantic water masses. Geochem. Geophys. Geosyst. 9, 18 PP.

Murphy, L.N., Kirk-Davidoff, D.B., Mahowald, N., Otto-Bliesner, B.L., 2009. A numerical study of the climate response to lowered Mediterranean Sea level during the Messinian Salinity Crisis. Palaeogeography, Palaeoclimatology, Palaeoecology 279, 41–59.

New, A., Barnard, S., Herrmann, P., Molines, J.-M., 2001. On the origin and pathway of the saline inflow to the Nordic Seas: insights from models. Progress In Oceanography 48, 255–287.

Pahnke, K., van de Flierdt, T., Jones, K.M., Lambelet, M., Hemming, S.R., Goldstein, S.L., 2012. GEOTRACES intercalibration of neodymium isotopes and rare earth element concentrations in seawater and suspended particles. Part 2: Systematic tests and baseline profiles. Limnology and Oceanography: Methods 10, 252–269.

Palmer, M.., Elderfield, H., 1986. Rare earth elements and neodymium isotopes in ferromanganese oxide coatings of Cenozoic foraminifera from the Atlantic Ocean. Geochimica et Cosmochimica Acta 50, 409–417.

Palmer, M.R., Elderfield, H., 1985. Variations in the Nd isotopic composition of foraminifera from Atlantic Ocean sediments. Earth and Planetary Science Letters 73, 299–305.

Pena, L.D., Cacho, I., Calvo, E., Pelejero, C., Eggins, S., Sadekov, A., 2008. Characterization of contaminant phases in foraminifera carbonates by electron microprobe mapping. Geochem. Geophys. Geosyst. 9, 12 PP.

Pena, L.D., Calvo, E., Cacho, I., Eggins, S., Pelejero, C., 2005. Identification and removal of Mn-Mg-rich contaminant phases on foraminiferal tests: Implications for Mg/Ca past temperature reconstructions. Geochem. Geophys. Geosyst. 6, 25 PP.

Penaud, A., Eynaud, F., Sánchez-Goñi, M., Malaizé, B., Turon, J.L., Rossignol, L., 2011. Contrasting sea-surface responses between the western Mediterranean Sea and eastern subtropical latitudes of the North Atlantic during abrupt climatic events of MIS 3. Marine Micropaleontology 80, 1–17.

Pin, C., Zalduegui, J.F.S., 1997. Sequential separation of light rare-earth elements, thorium and uranium by miniaturized extraction chromatography: Application to isotopic analyses of silicate rocks. Analytica Chimica Acta 339, 79–89.

Piotrowski, A.M., Galy, A., Nicholl, J.A.L., Roberts, N., Wilson, D.J., Clegg, J.A., Yu, J., 2012. Reconstructing deglacial North and South Atlantic deep water sourcing using foraminiferal Nd isotopes. Earth and Planetary Science Letters 357–358, 289–297.

Pomiès, C., Davies, G.R., Conan, S.M.-H., 2002. Neodymium in modern foraminifera from the Indian Ocean: implications for the use of foraminiferal Nd isotope compositions in paleo-oceanography. Earth and Planetary Science Letters 203, 1031–1045.

Potemra, J.T., Hautala, S.L., Sprintall, J., 2003. Vertical structure of Indonesian throughflow in a large-scale model. Deep Sea Research Part II: Topical Studies in Oceanography 50, 2143–2161.

Rempfer, J., Stocker, T.F., Joos, F., Dutay, J.-C., 2012. Sensitivity of Nd isotopic composition in seawater to changes in Nd sources and paleoceanographic implications. J. Geophys. Res. 117, C12010.

Rempfer, J., Stocker, T.F., Joos, F., Dutay, J.-C., Siddall, M., 2011. Modelling Nd-isotopes with a coarse resolution ocean circulation model: Sensitivities to model parameters and source/sink distributions. Geochimica et Cosmochimica Acta 75, 5927–5950.

Richard, P., Allegre, C.J., 1980. Neodymium and strontium isotope study of ophiolite and orogenic lherzolite petrogenesis. Earth and Planetary Science Letters 47, 65–74.

Roberts, N.L., Piotrowski, A.M., Elderfield, H., Eglinton, T.I., Lomas, M.W., 2012. Rare earth element association with foraminifera. Geochimica et Cosmochimica Acta 94, 57–71.

Roberts, N.L., Piotrowski, A.M., McManus, J.F., Keigwin, L.D., 2010. Synchronous Deglacial Overturning and Water Mass Source Changes. Science 327, 75–78.

Roger, S., Münch, P., Cornée, J.J., Saint Martin, J.P., Féraud, G., Pestrea, S., Conesa, G., Ben Moussa, A., 2000. 40Ar/39Ar dating of the pre-evaporitic Messinian marine sequences of the Melilla basin (Morocco): a proposal for some biosedimentary events as isochrons around the Alboran Sea. Earth and Planetary Science Letters 179, 101–113.

Rogerson, M., Colmenero-Hidalgo, E., Levine, R.C., Rohling, E.J., Voelker, A.H.L., Bigg, G.R., Schönfeld, J., Cacho, I., Sierro, F.J., Löwemark, L., Reguera, M.I., Abreu, L. de, Garrick, K., 2010. Enhanced Mediterranean-Atlantic exchange during Atlantic freshening phases. Geochem. Geophys. Geosyst. 11, 22 PP.

Rogerson, M., Rohling, E.J., Bigg, G.R., Ramirez, J., 2012. Paleoceanography of the Atlantic-Mediterranean exchange: Overview and first quantitative assessment of climatic forcing. Rev. Geophys. 50, 32 PP.

Roveri, M., Lugli, S., Manzi, V., Schreiber, B.C., 2008. The Messinian Sicilian stratigraphy revisited: new insights for the Messinian salinity crisis. Terra Nova 20, 483–488.

Ryan, W.B.F., Hsu, K.J., et al., 1973. Initial Reports of the Deep Sea Drilling Project, 13. U.S. Government Printing Office.

Saint Martin, J.-P., Cornee, J.-J., 1996. The Messinian reef complex of Melilla, Northeastern Rif, Morocco, in: Franseen, E.K., Esteban, M., Ward, W.C., Rouchy, J.-M. (Eds.), Models for carbonate stratigraphy from Miocene reef complexes of Mediterranean regions, Concepts in Sedimentology and Paleontology.

Santisteban, C., Taberner, C., 1983. Shallow marine and continental conglomerates derived from coral reef complexes after desiccation of a deep marine basin: the Tortonian-

Messinian deposits of the Fortuna Basin, SE Spain. Journal of the Geological Society 140, 401–411.

Scher, H.D., Delaney, M.L., 2010. Breaking the glass ceiling for high resolution Nd isotope records in early Cenozoic paleoceanography. Chemical Geology 269, 329–338.

Scrivner, A.E., Vance, D., Rohling, E.J., 2004. New neodymium isotope data quantify Nile involvement in Mediterranean anoxic episodes. Geology 32, 565 –568.

Sholkovitz, E.R., 1989. Artifacts associated with the chemical leaching of sediments for rare-earth elements. Chemical Geology 77, 47–51.

Sierro, F.J., Flores, J.A., Francés, G., Vazquez, A., Utrilla, R., Zamarreño, I., Erlenkeuser, H., Barcena, M.A., 2003. Orbitally-controlled oscillations in planktic communities and cyclic changes in western Mediterranean hydrography during the Messinian. Palaeogeography, Palaeoclimatology, Palaeoecology 190, 289–316.

Sierro, F.J., Hilgen, F.J., Krijgsman, W., Flores, J.A., 2001. The Abad composite (SE Spain): a Messinian reference section for the Mediterranean and the APTS. Palaeogeography, Palaeoclimatology, Palaeoecology 168, 141–169.

Spivack, A.J., Wasserburg, G.., 1988. Neodymium isotopic composition of the Mediterranean outflow and the eastern North Atlantic. Geochimica et Cosmochimica Acta 52, 2767–2773.

Sprintall, J., Wijffels, S.E., Molcard, R., Jaya, I., 2009. Direct estimates of the Indonesian Throughflow entering the Indian Ocean: 2004–2006. J. Geophys. Res. 114, 19 PP.

Staudigel, H., Doyle, P., Zindler, A., 1985. Sr and Nd isotope systematics in fish teeth. Earth and Planetary Science Letters 76, 45–56.

Stumpf, R., Frank, M., Schönfeld, J., Haley, B.A., 2011. Climatically driven changes in sediment supply on the SW Iberian shelf since the Last Glacial Maximum. Earth and Planetary Science Letters 312, 80–90.

Tachikawa, K., Athias, V., Jeandel, C., 2003. Neodymium budget in the modern ocean and paleo-oceanographic implications. J. Geophys. Res. 108, 1–13.

Tachikawa, K., Jeandel, C., Roy-Barman, M., 1999. A new approach to the Nd residence time in the ocean: the role of atmospheric inputs. Earth and Planetary Science Letters 170, 433–446.

Tachikawa, K., Roy-Barman, M., Michard, A., Thouron, D., Yeghicheyan, D., Jeandel, C., 2004. Neodymium isotopes in the Mediterranean Sea: comparison between seawater and sediment signals. Geochimica et Cosmochimica Acta 68, 3095–3106.

Thomas, D.J., Bralower, T.J., Jones, C.E., 2003. Neodymium isotopic reconstruction of late Paleocene–early Eocene thermohaline circulation. Earth and Planetary Science Letters 209, 309–322.

Topper, R.P.M., Flecker, R., Meijer, P.T., Wortel, M.J.R., 2011. A box model of the Late Miocene Mediterranean Sea: Implications from combined 87Sr/86Sr and salinity data. Paleoceanography 26, PA3223.

Tsimplis, M.N., Bryden, H.L., 2000. Estimation of the transports through the Strait of Gibraltar. Deep Sea Research Part I Oceanographic Research Papers 47, 2219–2242.

van Assen, E., Kuiper, K.F., Barhoun, N., Krijgsman, W., Sierro, F.J., 2006. Messinian astrochronology of the Melilla Basin: Stepwise restriction of the Mediterranean-Atlantic connection through Morocco. Palaeogeography, Palaeoclimatology, Palaeoecology 238, 15–31.

van de Flierdt, T., Frank, M., Lee, D.-C., Halliday, A.N., Reynolds, B.C., Hein, J.R., 2004. New constraints on the sources and behavior of neodymium and hafnium in seawater from Pacific Ocean ferromanganese crusts. Geochimica et Cosmochimica Acta 68, 3827–3843.

van der Laan, E., Snel, E., Kaenel, E. de, Hilgen, F.J., Krijgsman, W., 2006. No major deglaciation across the Miocene-Pliocene boundary: Integrated stratigraphy and astronomical tuning of the Loulja sections (Bou Regreg area, NW Morocco). Paleoceanography 21, 27 PP.

Vance, D., Burton, K., 1999. Neodymium isotopes in planktonic foraminifera: a record of the response of continental weathering and ocean circulation rates to climate change. Earth and Planetary Science Letters 173, 365–379.

Vance, D., Scrivner, A.E., Beney, P., Staubwasser, M., Henderson, G.M., Slowey, N.C., 2004. The use of foraminifera as a record of the past neodymium isotope composition of seawater. Paleoceanography 19, 17 PP.

Via, R.K., Thomas, D.J., 2006. Evolution of Atlantic Thermohaline Circulation: Early Oligocene Onset of Deep-Water Production in the North Atlantic. Geology 34, 441–444.

Wagner, C., Mokhtari, A., Deloule, E., Chabaux, F., 2003. Carbonatite and Alkaline Magmatism in Taourirt (Morocco): Petrological, Geochemical and Sr–Nd Isotope Characteristics. J. Petrology 44, 937–965.

Figures

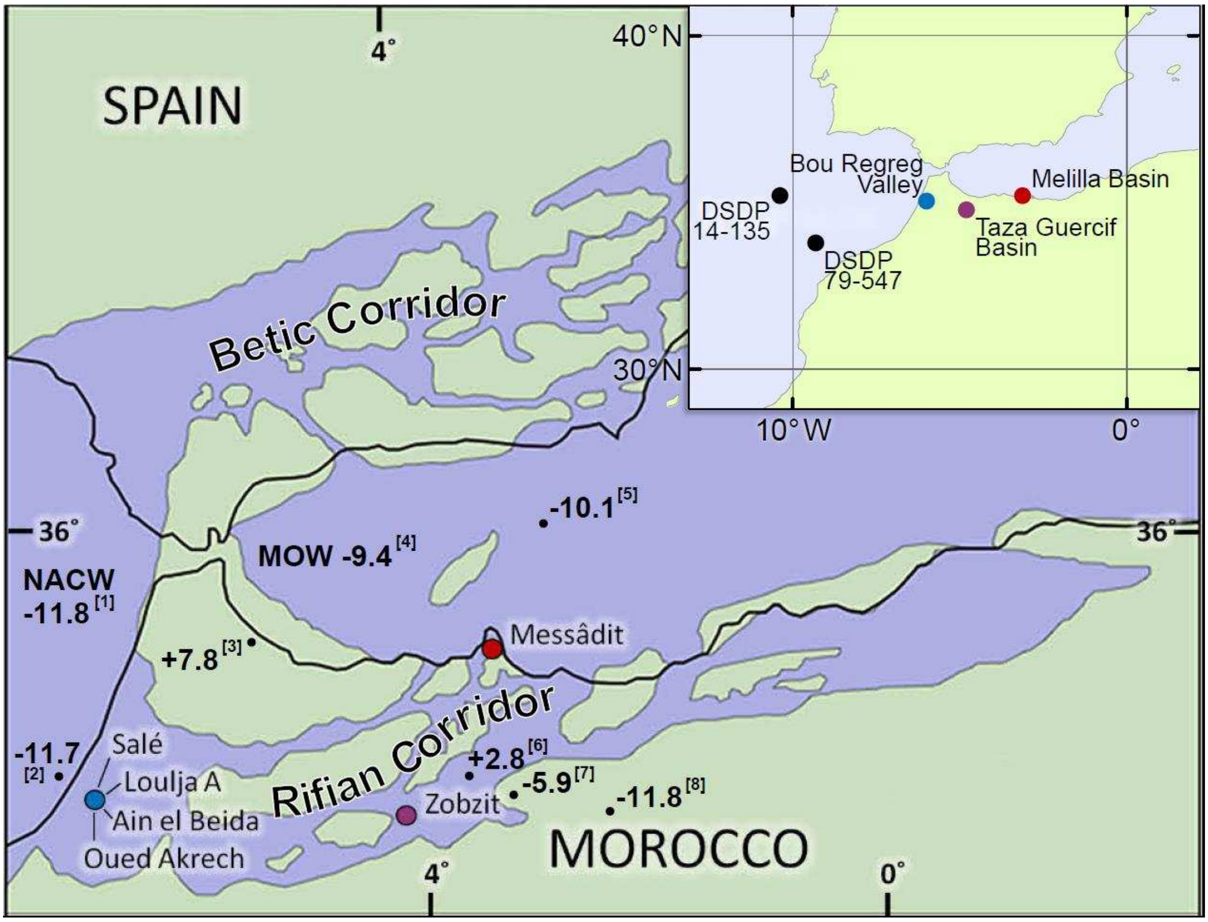

Figure 1. Location map of the Rifian (Moroccan) Corridor sample sites. The modern coastline is indicated by a black line, late Miocene land is shaded green and late Miocene ocean is shaded blue. Numbers in bold represent $\varepsilon_{Nd(T)}$ (see text) measured in; [1] modern seawater associated with North Atlantic Central Water (multi-sample mean, all -11.8 approx.; Spivack and Wasserburg, 1988), [2] the detrital fraction of seafloor surface sediment (one sample; Grousset et al., 1998), [3] lherzolite from an ultramafic complex (mean of two samples; 2.2 and 13.5 approx.; Richard and Allegre, 1980), [4] modern seawater associated with Mediterranean Outflow Water (multi-sample mean with range -9.6 to -9.2 approx.; Spivack and Wasserburg, 1988; Henry et al., 1994; Tachikawa et al., 2004), [5] the detrital fraction of seafloor surface sediment (one sample; Grousset et al., 1988), [6] bulk rock from an alkaline-carbonatite complex of lamprophyre dykes (multi-sample mean with range 0.3 to 4.5 approx.; Wagner et al., 2003), [7] bulk rock from a calc-alkaline complex (multi-sample

mean with range -14.8 to 4.1 approx.; Ajaji et al., 1998) and [8] loess (Grousset et al., 1998). The corridor reconstruction is based on Santisteban and Taberner (1983).

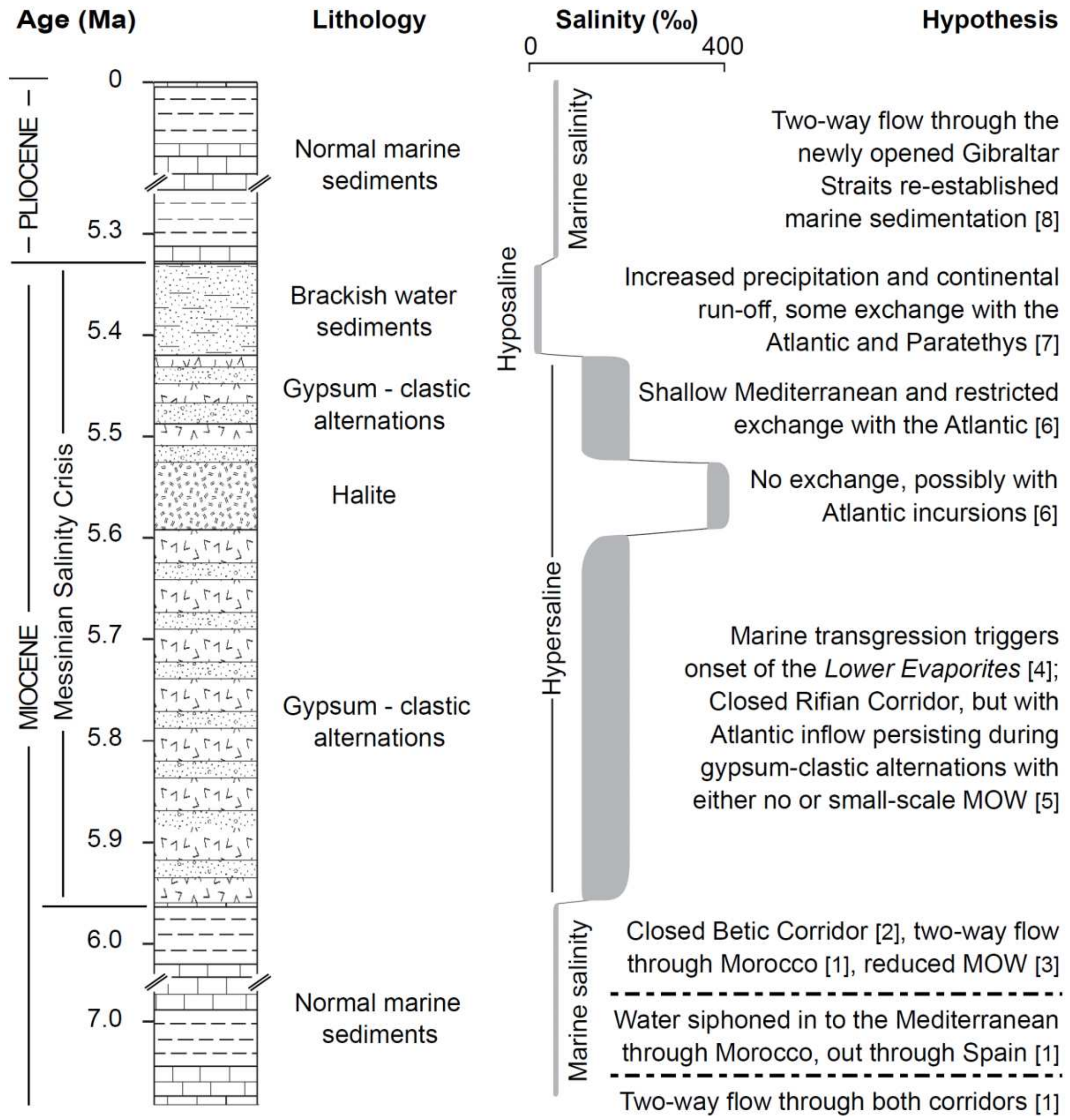

Figure 2. Schematic composite section of the main Mediterranean lithologies over the Messinian Salinity Crisis, including the corresponding salinities in which the successions were deposited/precipitated (timings of event boundaries are after Roveri et al., 2008 and references therein). Also shown are the hypotheses for changes in Mediterranean-Atlantic water exchange (and Mediterranean Outflow Water, MOW), which have been put forward to explain the extreme salinity fluctuations. The numbers in square brackets indicate the references for these; [1] Benson et al. (1991), [2] Martin et al. (2001), [3] Flecker and Ellam (2006), [4] Flecker et al. (2002), [5] Krijgsman et al. (2008), [6] Roveri et al. (2008), [7] Carnevale et al. (2006), and [8] Hsu et al. (1973a; 1973b).

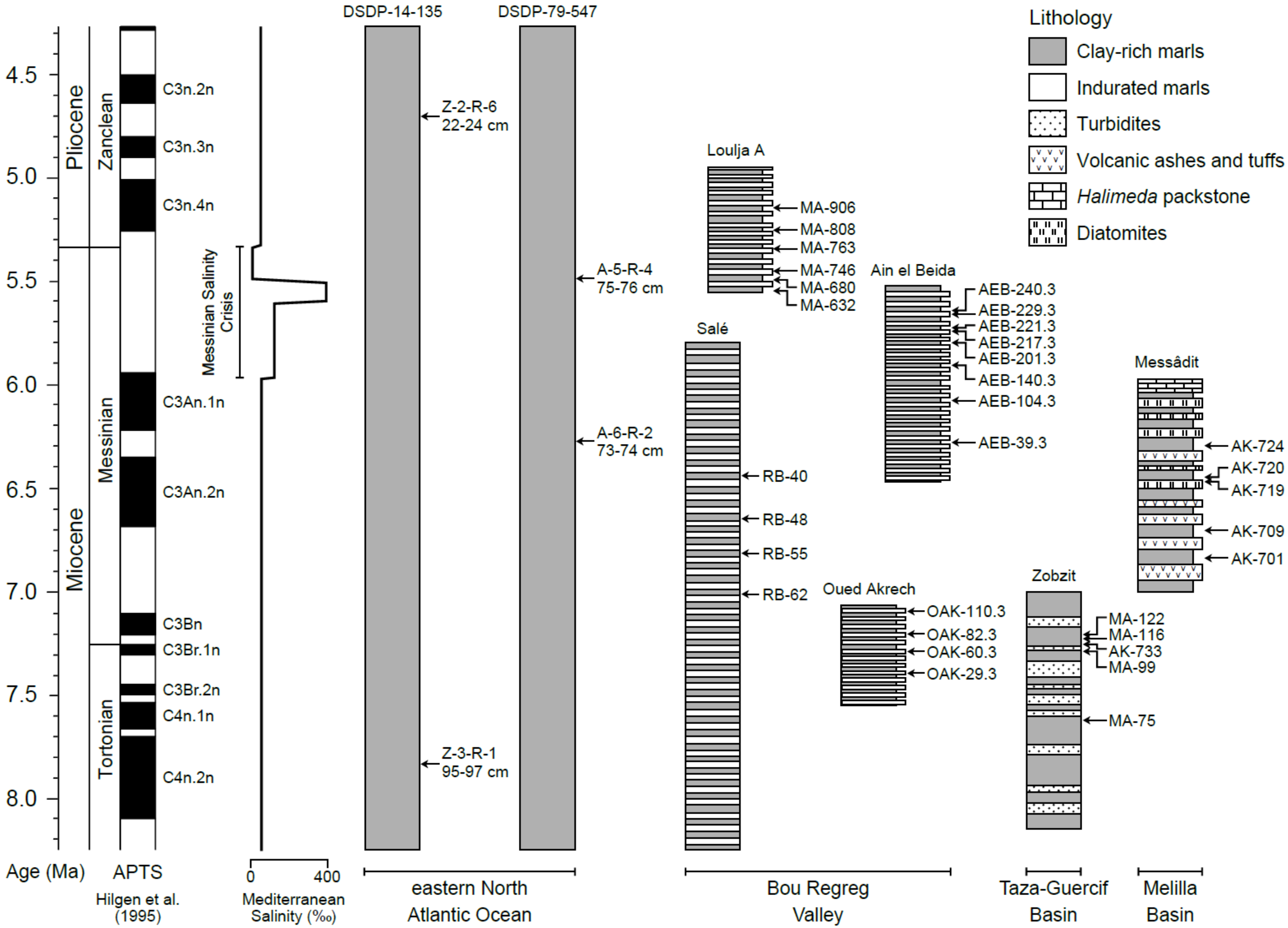

DSDP-14-135
DSDP-79-547
Lithology
Clay-rich marls
Indurated marls
Turbidites
Volcanic ashes and tuffs
Halimeda packstone
Diatomites
Pliocene
Zanclean
Miocene
Messinian
Tortonian
C3n.2n
C3n.3n
C3n.4n
C3An.1n
C3An.2n
C3Bn
C3Br.1n
C3Br.2n
C4n.1n
C4n.2n
Messinian Salinity Crisis
Z-2-R-6 22-24 cm
A-5-R-4 75-76 cm
A-6-R-2 73-74 cm
Z-3-R-1 95-97 cm
Loulja A
MA-906
MA-808
MA-763
MA-746
MA-680
MA-632
Ain el Beida
AEB-240.3
AEB-229.3
AEB-221.3
AEB-217.3
AEB-201.3
AEB-140.3
AEB-104.3
AEB-39.3
Salé
RB-40
RB-48
RB-55
RB-62
Messâdit
AK-724
AK-720
AK-719
AK-709
AK-701
Oued Akrech
OAK-110.3
OAK-82.3
OAK-60.3
OAK-29.3
Zobzit
MA-122
MA-116
AK-733
MA-99
MA-75
Age (Ma)
APTS
Hilgen et al. (1995)
0
400
Mediterranean Salinity (‰)
eastern North Atlantic Ocean
Bou Regreg Valley
Taza-Guercif Basin
Melilla Basin

Figure 3. Schematic stratigraphy of all sample cores and sections (locations indicated on Fig. 1), annotated with sample numbers. The magnetic polarity is from Hilgen et al. (1995); black and white intervals represent normal and reversed polarity, respectively. References for the stratigraphies and age models are given in Supplementary Tables S1 and S2, alongside more detailed descriptions of the sampled lithologies. Approximate Mediterranean salinity and the Messinian Salinity Crisis are also shown.

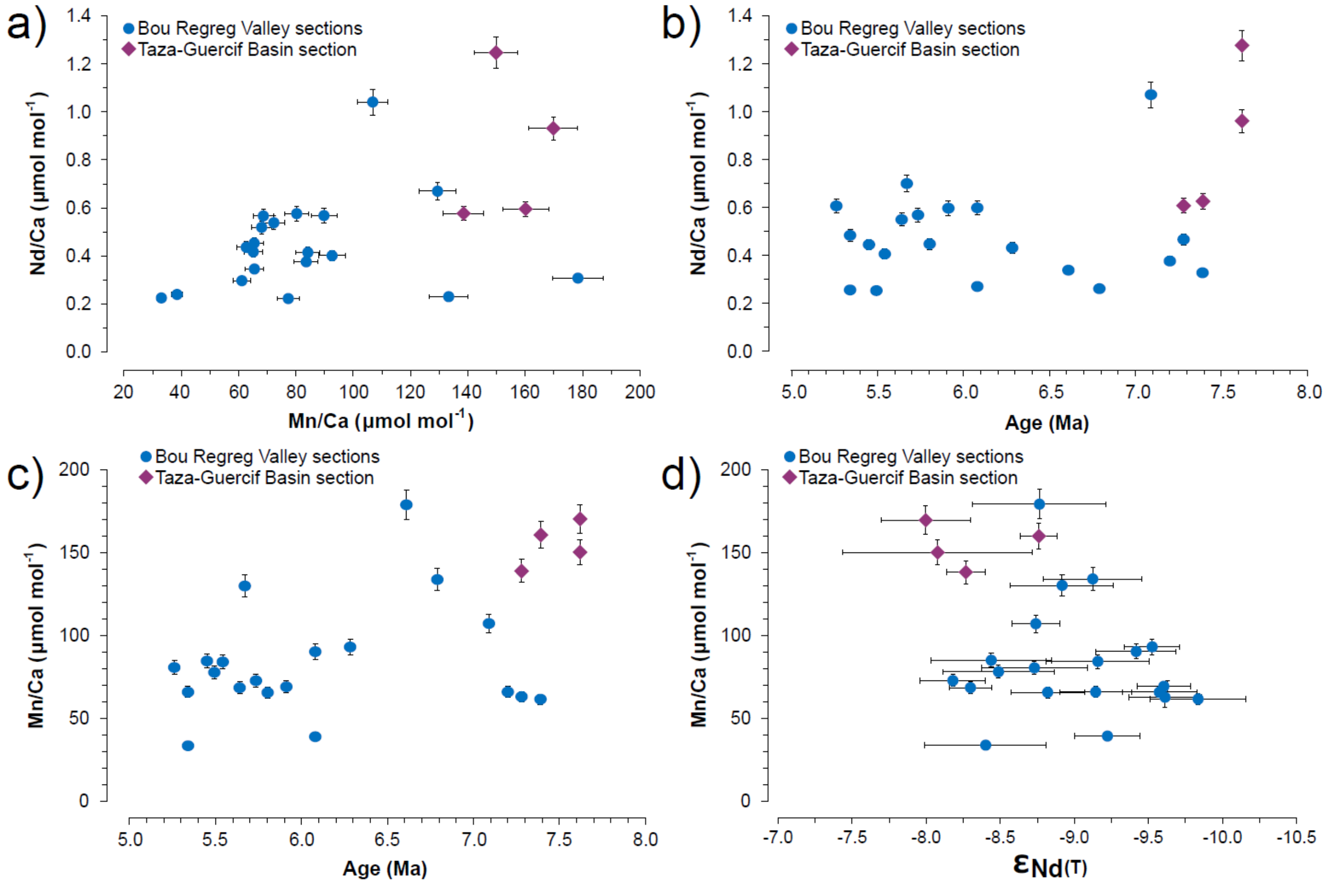

Figure 4. (a) Nd/Ca ratios and Mn/Ca ratios, (b) Nd/Ca ratios and sample age, (c) Mn/Ca ratios and $\varepsilon_{Nd(T)}$ and (d) Mn/Ca ratios and sample of all benthic foraminifera material; note that there is no benthic foraminifera data from Messâdit, DSDP-14-135 and DSDP-79-547 sediments. All element/Ca ratios are shown with a precision of 5 %. $\varepsilon_{Nd(T)}$ measurements are shown with an internal error of 2 standard errors from the mean, if larger than external reproducibility, based on La Jolla standard $^{143}Nd/^{144}Nd$. Samples from the Zobzit section generally have higher Nd/Ca and Mn/Ca ratios than samples from the more westerly Bou Regreg Valley (Salé, Loulja A, Ain el Beida and Oued Akrech), possibly due to Zobzit's palaeo-proximity to the continent making it more susceptible to fluvial and aeolian influence (Fig. 1, see text, section 3.1). There is no statistically significant correlation between Nd/Ca and Mn/Ca, between Nd/Ca or Mn/Ca and age, or between Mn/Ca and $\varepsilon_{Nd(T)}$.

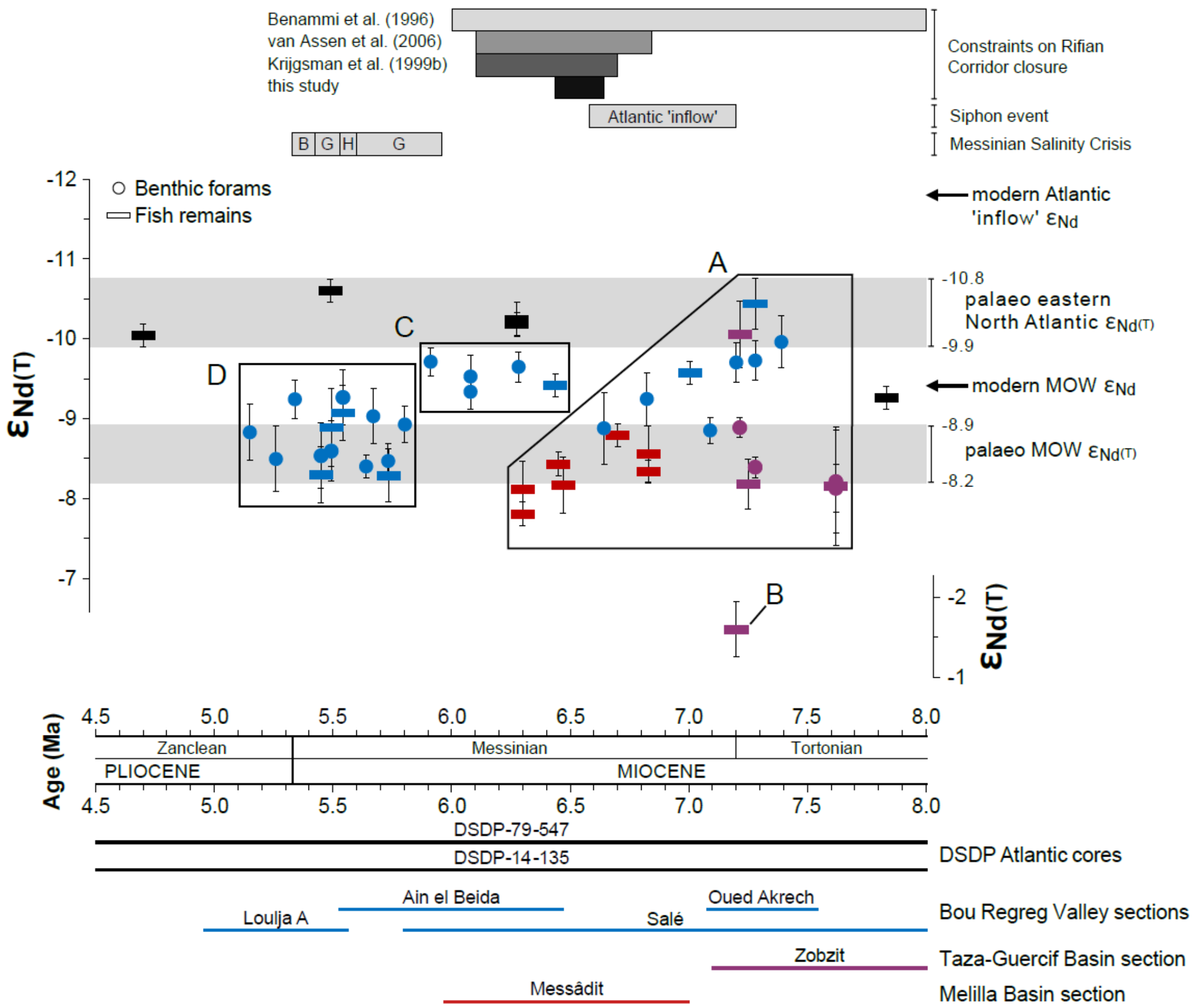

Figure 5. Mean $\varepsilon_{Nd(T)}$ (with internal error of ±2 standard deviations from the mean if larger than external reproducibility) measured in sedimentary benthic foraminifera and fossil fish remains (bones and teeth) from the eight ocean and terrestrial sample sites (Figures 1 and 3) plotted against sample age. Note that sample ages for DSDP-14-135 and DSDP-79-547 are very approximate (section 2.2). The data marked by Boxes A, C and D and by Excursion B are described in the text. For the Messinian Salinity Crisis events in the Mediterranean, 'B' indicates the phase of Lago Mare (brackish water) conditions, 'G' indicates gypsum precipitation and 'H' indicates halite precipitation; timings after Roveri et al. (2008). Modern Mediterranean Outflow Water (MOW) and Atlantic inflow $\varepsilon_{Nd(T)}$ were measured by Spivack and Wasserburg (1988), Henry et al. (1994) and Tachikawa et al. (2004).

Supplementary Material

Table S1. Details of sample sites. The locations of the cores and sections are shown in Fig. 1. See Table S2 for sample ages and lithologies.

Table S2. Sample log. For cored sediments^ the depth from the core-top is given, for exposed terrestrial sections* the stratigraphic height from the section-base is given. For the palaeo-Nd archives, ‘foraminifera’ has been shortened to ‘foram.’ and ‘fragments’ to ‘frag.’. All picked material was >150 μm; the fraction of material >250 μm is shown alongside the total counts. For the lithologies, the marls are clay-rich, often slightly reddish and susceptible to weathering. The indurated marls are carbonate-rich, light coloured, well cemented and often protuberant as they are more resistant to weathering than the adjacent marls. One sample (AK-719, Messâdit) is taken from a white, well-developed, finely laminated (1-3 mm thick laminations) diatomite, which is rich in ostracods and bivalves. High resolution, astronomically-tuned age models are available for the Rifian Corridor sections, yielding accurate age constraints; Salé (Hodell et al., 1994, but using the revised age model of Gradstein et al., 2005), Loulja A (van der Laan et al., 2006), Ain el Beida (Krijgsman et al., 2004), Oued Akrech (Hilgen et al., 2000), Zobzit (Krijgsman et al., 1999b) and Messâdit (van Assen et al., 2006). DSDP sample ages have been approximated according to the low resolution, biostragraphy-based aged models presented by Hayes et al. (1972) and Hinz et al. (1984).

Table S3. Mean Nd and Sm isotope ratios. $^{143}Nd/^{144}Nd$ isotope ratios are given ± their reproducibility (× 10^6), $\varepsilon_{Nd(T)}$ are reported ±their internal precision (two standard errors from the mean; 2σ) and $^{147}Sm/^{144}Sm$ isotope ratios are given ±their 2σ internal precision (× 10^4). The Nd ratios have been corrected for machined-induced mass bias relative to pure La Jolla and Ce-spiked La Jolla Nd standards as well as for ^{147}Sm decay to ^{143}Nd; ε_{Nd} denotes the raw ratios, $\varepsilon_{Nd(T)}$ denotes the ^{143}Nd ingrowth-corrected ratios. The Sm ratios have been corrected for machined-induced mass bias relative to a natural $^{147}Sm/^{149}Sm$ of 1.08507.

Table S4. Element/Ca ratios for mixed benthic foraminifera samples reported alongside mean Nd isotope ratios (expressed in terms of $\varepsilon_{Nd(T)}$ ±2 standard errors from the mean; 2σ). $\varepsilon_{Nd(T)}$ denotes the post-depositional ingrowth of ^{143}Nd-corrected ε_{Nd}.

Figure S1. Foraminifera and fish tooth-derived Nd isotopic compositions plotted as $\varepsilon_{Nd(T)}$ (±2 standard errors from the mean; 2σ) versus procedural blank Nd contribution to the sample (shown in %) . This has been calculated by comparing the concentration of Nd measured in each sample to the concentration of Nd measured in the total procedural blank run in the same analytical session. $\varepsilon_{Nd(T)}$ denotes the post-depositional ingrowth of ^{143}Nd-corrected ε_{Nd}. No clearly offsetting effect with increasing blank contributions is resolvable.